

# Amorphous structure changes in poly(ethylene terephthalate) induced by annealing under dry and wet conditions and its dye uptake properties

Tamako Toda\*

Showa Women's Junior College, Tokyo 154, Japan

Hirohisa Yoshida

Department of Industrial Chemistry, Tokyo Metropolitan University, Tokyo 192-03, Japan

and Koushi Fukunishi

Department of Chemistry and Materials Technology, Kyoto Institute of Technology, Kyoto 606, Japan

(Received 16 October 1995; revised 3 October 1996)

The amorphous structure changes in poly(ethylene terephthalate) (PET) induced by annealing under dry and wet conditions were discussed in terms of amorphous density ( $\rho_a$ ) and dye uptake properties. The  $\rho_a$  value of PET decreased with increasing annealing temperature, but it conversely increased at annealing temperatures above 210°C for the dry treatment and above 170°C for the wet treatment. With decreasing  $\rho_a$  from 1.35 to 1.31 g cm<sup>-3</sup>, the conformation of amorphous molecules changed from the *gauche* to *trans* form. The  $\rho_a$  value conversely increased on annealing at higher temperatures; however, the dye exhaustion continuously increased. The ratio of the absorbance of the  $\alpha$  band to that of the  $\beta$  band of the basic dye crystal violet ( $\alpha/\beta$  ratio), indicating the degree of dye aggregation, in PET decreased with a decrease in  $\rho_a$ . The degree of dye aggregation further increased when  $\rho_a$  conversely increased on high temperature annealing. These results suggested that the free volume content of PET increased as a result of conformational change from the *gauche* to *trans* form in amorphous molecules with increasing annealing temperature, and finally the increased free volume converted to microvoids around 1.31 g cm<sup>-3</sup> of  $\rho_a$ . The dye exhaustion increased with increasing annealing temperature according to microvoid formation. © 1997 Elsevier Science Ltd.

(Keywords: poly(ethylene terephthalate); amorphous structure; amorphous density)

## INTRODUCTION

It is well known that the isothermal sorption of disperse dyes in various annealed poly(ethylene terephthalate) (PET) fibres at a constant dyeing time usually shows a very characteristic behaviour. Marvin<sup>1</sup> was the first to show that, over a range of annealing temperatures, the disperse dye uptake of annealed PET fibres initially decreased as the annealing temperature increased, and then it increased to over the value of the untreated control at higher annealing temperatures. Since it is generally accepted that dye sorption mainly takes place in the amorphous region of a polymer, this dyeing phenomenon is supposed to be brought about by changes in the amorphous region during annealing. In other words, the physical state of the dye in the polymer affords information on the amorphous structure. Several attempts<sup>2-7</sup> were made to explain the variations in dyeing properties in terms of structural change in the polymer, e.g. crystal size, thickness of amorphous region between

crystal lamellae, amorphous orientation, void and dynamic loss modulus of materials. An increase in dye uptake with increasing annealing temperature was interpreted as an increase in the accessibility of the dye molecule<sup>5-7</sup>. Some explanations were presented to give the relationship between the amount of dye sorption and fine structure parameters of polymer, derived on the assumption that dye sorption takes place only on the surfaces of crystallites<sup>8-10</sup>. The theoretical analysis of the experimental data implied that sorption sites were located more densely near crystal surfaces than in the interior of the amorphous region<sup>8</sup>. Yonetake and co-workers<sup>9,10</sup> proposed a sorption model based on the idea that disperse dyes were dissolved in two kinds of amorphous regions: the end and side surfaces of crystal lamella.

In most studies, as mentioned above, the relationship between the dye exhaustion and the amorphous structure was not directly and quantitatively discussed sufficiently; therefore, the dye uptake behaviour has not yet been explained in detail. We believe that the dye uptake behaviour must be explained from the viewpoint of the amorphous structure of PET and of the absorption state

\*To whom correspondence should be addressed

of dyes in PET. In our previous paper<sup>11</sup> the amorphous structure of PET was investigated using small and wide angle X-ray diffraction (WAXD) methods, density measurements, differential scanning calorimetry (d.s.c.) and dynamic viscoelastic measurements. The degree of crystallinity increased with an increase in annealing temperature. From the observed values of density and crystallinity evaluated from the transmission WAXD, the amorphous density was calculated assuming a constant density of the crystalline region. The calculated amorphous density decreased as crystallization proceeded. On the other hand, the glass transition temperature, the apparent activation energy and the relaxation strength of  $\alpha$  relaxation decreased with an increase in annealing temperature. These facts suggested that molecular motion in the amorphous region easily occurred and the number of molecules responsible for the glass transition decreased as crystallization proceeded. The structure of the amorphous region, therefore, became sparse due to annealing. Water molecules enhanced the segmental mobility of PET and the structural changes during the crystallization of PET. Structural difference was observed between PET samples annealed under dry and wet conditions.

In this study, interpretation of the amorphous structure changes in PET induced by annealing under dry and wet conditions is attempted in terms of amorphous density and dye uptake properties. Interpretation of the characteristic dyeing behaviour of annealed PET fibres, which was first found by Marvin<sup>1</sup>, has been attempted so far in terms of crystallinity or dye sorption sites of crystal surfaces. The dyeing behaviour of PET annealed under dry and wet conditions is also discussed in terms of amorphous structure in this study.

## EXPERIMENTAL

### Sample

The extruded PET, a 9  $\mu\text{m}$  thick film, manufactured by Teijin Co. Ltd., was used throughout the experiments. The density of the original PET film was  $1.4015 \text{ g cm}^{-3}$  at  $23^\circ\text{C}$ . The degree of crystallinity of the original PET determined by the WAXD method was 0.34, which agreed with the value evaluated by the heat of fusion<sup>11</sup>. PET samples were annealed at various temperatures from 100 to  $230^\circ\text{C}$  for 1 h under a dry nitrogen atmosphere (dry annealing) or in water (wet annealing). After annealing, PET samples were cooled down to room temperature and stored in a desiccator over diphosphorus pentoxide.

### Dye sorption

As reported in our previous paper<sup>12</sup>, equilibrium sorption was not established in the long-term dyeing, because the films, which were annealed under several wet conditions or under dry and high temperature conditions, were broken into small pieces during dyeing. Therefore, a dyeing time of 8 h was chosen as the condition of equilibrium sorption, which was obtained by about 7 h dyeing in this investigation. PET films were dyed with  $1.754 \times 10^{-4} \text{ mol l}^{-1}$  of crystal violet chloride (C.I. Basic Violet 3; CV) solution at  $110^\circ\text{C}$  for 8 h in a liquor ratio of 1250:1 under pressure. It was recognized that the films were dyed uniformly by observation of cross-sections of dyed films under a light microscope. The pH of the dye solution was 6.0. All dyed films were

successively washed with water and ethanol in order to remove any excess dye on the film surface and were then air-dried at room temperature. The adsorbed dye was extracted with ethanol, and the dye concentration was determined using a spectrophotometric method<sup>13</sup>.

### Measurements

PET densities were measured in a density gradient column containing a mixture of n-heptane and carbon tetrachloride at  $23 \pm 0.1^\circ\text{C}$  as reported previously<sup>11</sup>. The error of density measurements was at most  $\pm 0.2\%$ .

WAXD profiles of PET were measured using a Mac Science model SRA MXP-18 X-ray instrument operating at 40 kV and 300 mA. Monochromated X-ray radiation was used and the X-ray wavelength was 0.15405 nm. In order to eliminate the surface orientation effect of crystallites, the sample was wound tightly and attached to a fibre sample holder to determine the degree of crystallinity in the transmission mode. Samples were rotated at  $10 \text{ rev min}^{-1}$  during the measurements in order to eliminate the biaxial orientation effect, and a radial diffractometer scanned in the  $2\theta$  range from  $5$  to  $60^\circ$  in the step-scanning mode. The raw data were subjected to background subtraction, and to polarization, absorption and incoherent scattering corrections.

Small angle X-ray scattering (SAXS) profiles were measured using SAXS optics installed at BL-10C at the photon factory of the National Laboratory for High Energy Physics, Tsukuba, Japan. The X-ray wavelength was selected by a double crystal monochromator and was fixed at 0.1488 nm. WAXD and SAXS were measured at  $23^\circ\text{C}$ .

The thermal properties of PET were measured using a Seiko differential scanning calorimeter DSC 200 connected to a Seiko thermal analysis system SSC 5000 equipped with a cooling apparatus. The d.s.c. heating curves were measured at  $10^\circ\text{C min}^{-1}$  in the temperature range  $0$ – $300^\circ\text{C}$  under dry nitrogen gas flow. The sample weight was about 4 mg. Temperature and enthalpy were calibrated using pure indium and tin. The degree of crystallinity was also evaluated from the heat of fusion measured by d.s.c. ( $X_{\text{d.s.c.}}$ ). This method is based on a thermodynamic definition of order and it requires the absolute value of the heat of fusion of the fully crystalline polymer,  $\Delta H_{\text{m}0} = 119.8 \text{ J g}^{-1}$  (ref. 14).  $X_{\text{d.s.c.}}$ , expressed as a weight fraction, can be determined as follows:  $X_{\text{d.s.c.}} = \Delta H_{\text{m,obs}} / \Delta H_{\text{m}0}$ .

The dynamic viscoelastic properties of PET were measured using a Seiko dynamic mechanical spectrometer DMS 200 connected to a Seiko material analysis station MAS 5700. Dynamic viscoelastic spectra were measured in the tension mode at 0.1, 0.2, 0.5, 1, 2, 5 and 10 Hz in the temperature range  $23$ – $200^\circ\text{C}$  heated at  $1^\circ\text{C min}^{-1}$ .

Fourier transform infra-red (FTi.r.) measurements were carried out using a Nicolet FTi.r. spectrophotometer system 800 with  $2 \text{ cm}^{-1}$  resolution at room temperature.

## RESULTS AND DISCUSSION

### Amorphous structure change

We evaluated the degree of crystallinity ( $X_c$ ) from WAXD profiles using a method proposed by Sakaguchi et al.<sup>15</sup>. They reported that correlation between the degrees of crystallinities of annealed unoriented PET

films determined from X-ray diffraction and density gave essentially a linear relationship which did not intersect the origin. The crystallinity evaluated from WAXD profiles using their method was reliable. Figure 1 shows changes in crystallinity values evaluated from the density ( $X_d$ ) and the d.s.c. ( $X_{d.s.c.}$ ) with  $X_c$  values for PET annealed under dry and wet conditions. For PET films annealed under both conditions, most of the data for  $X_{d.s.c.}$  were correlated to  $X_c$  by a linear relationship. On the other hand, for dry annealed PET, the relationship between  $X_d$  and  $X_c$  gave two linear lines, and one line parallel to the  $X_{d.s.c.}$ - $X_c$  relationship below a  $X_c$  value of 0.5. For the  $X_c$  range above 0.5 of dry annealed PET,  $X_d$  was almost a constant with increasing  $X_c$  value. For wet annealed PET, the data for  $X_d$  were correlated with  $X_c$  by two linear relationships which intersected at about 0.5 of  $X_c$ ; however, neither linear lines were parallel to the  $X_{d.s.c.}$ - $X_c$  relationship. This result suggested that the amorphous density of the PET film used in this study decreased on annealing because the crystal density could be assumed to be constant as previously reported<sup>11</sup>, and amorphous structure difference existed between dry and wet conditions.

As discussed in the previous paper<sup>11</sup>, the amorphous density ( $\rho_a$ ) of annealed PET was evaluated according to the following equation:

$$\rho_a = \rho \rho_c (1 - X_c) / (\rho_c - \rho X_c) \quad (1)$$

where  $\rho$ ,  $\rho_c$  and  $X_c$  indicated the measured density, the density of the crystalline phase ( $\rho_c = 1.4895 \text{ g cm}^{-3}$ )<sup>16,17</sup> and the degree of crystallinity evaluated by the WAXD measurements in the transmission mode<sup>11</sup>, respectively. Figure 2 shows changes in  $\rho_a$  with annealing temperature for PET annealed under dry and wet conditions. The  $\rho_a$  value decreased with increasing annealing temperature for both conditions, but it conversely increased at annealing temperatures above 210°C for the dry treatment and above 170°C for the wet treatment. For both annealing conditions,  $\rho_a$  changed according to the following three regions: region 1 ( $\rho_a > 1.35 \text{ g cm}^{-3}$ );  $\rho_a$  gradually decreased with increasing annealing temperature. Region 2 ( $1.35 \text{ g cm}^{-3} > \rho_a > 1.31 \text{ g cm}^{-3}$ );  $\rho_a$  greatly decreased with increasing annealing temperature. Region 3 ( $\rho_a > 1.31 \text{ g cm}^{-3}$ );  $\rho_a$  increased conversely

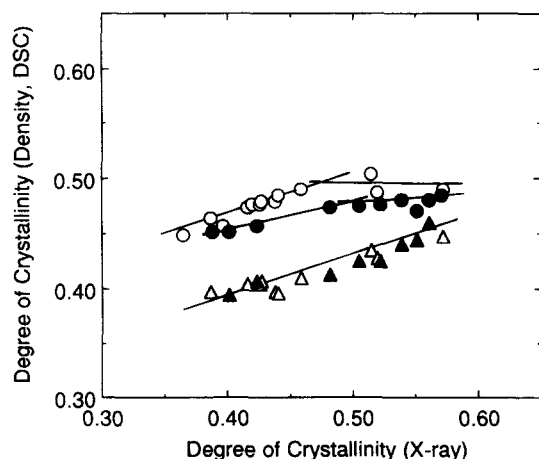


**Figure 1** Changes in crystallinity evaluated by density ( $X_d$ : dry,  $\circ$ ; wet,  $\bullet$ ) and ( $X_{d.s.c.}$ : dry,  $\triangle$ ; wet,  $\blacktriangle$ ) with crystallinity evaluated by transmission WAXD ( $X_c$ ) for PET annealed under dry and wet conditions

with increasing annealing temperature. Compared with the dry annealing condition, the transformation from region 1 to region 2 and from region 2 to region 3 was observed at lower annealing temperatures under the wet annealing condition as a result of the plasticizing effect of water. The minimum value of  $\rho_a$  ( $1.31 \text{ g cm}^{-3}$ ) was observed for the dry-210°C annealed and the wet-170°C annealed PET at the corresponding annealing condition.

Figure 3 shows the relationship between amorphous content ( $1 - X_c$ ) and  $\rho_a$  for both annealing conditions. For both annealing conditions,  $\rho_a$  data were classified into the three regions depicted in Figure 2. For wet annealed PET, all data belonging to regions 1, 2 and 3 were correlated with amorphous content by three linear relationships in each region. The two linear relationships intersected at  $1.34 \text{ g cm}^{-3}$ , which was close to the widely noted typical value of  $\rho_a$  ( $1.3379 \text{ g cm}^{-3}$ ) of PET<sup>18,19</sup>. Only two data points belonged to region 2 for dry annealed PET; however, a similar linear extrapolation of data belonging to regions 1-3 gave  $1.345 \text{ g cm}^{-3}$  as the intersection. This value was also close to the typical value of  $\rho_a$  of PET. These results suggested that the amorphous structure differed from region to region. As the occupied volume of molecular chains in the amorphous region was

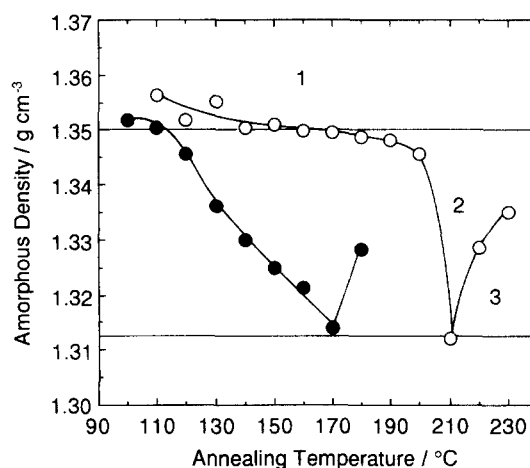


**Figure 2** Changes in amorphous density ( $\rho_a$ ) of PET annealed under dry ( $\circ$ ) and wet ( $\bullet$ ) conditions as a function of annealing temperature

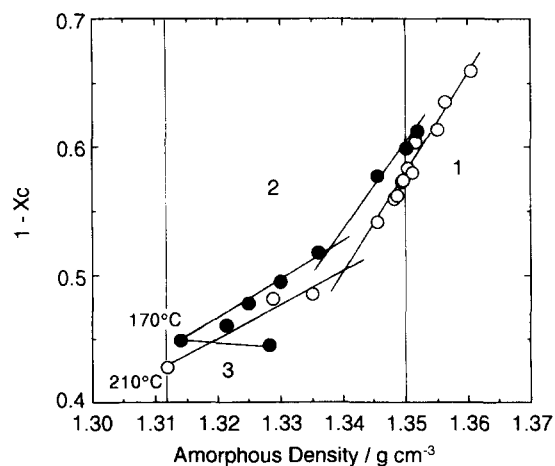


**Figure 3** Relationship between amorphous content ( $1 - X_c$ ) and amorphous density ( $\rho_a$ ) in PET annealed under dry ( $\circ$ ) and wet ( $\bullet$ ) conditions

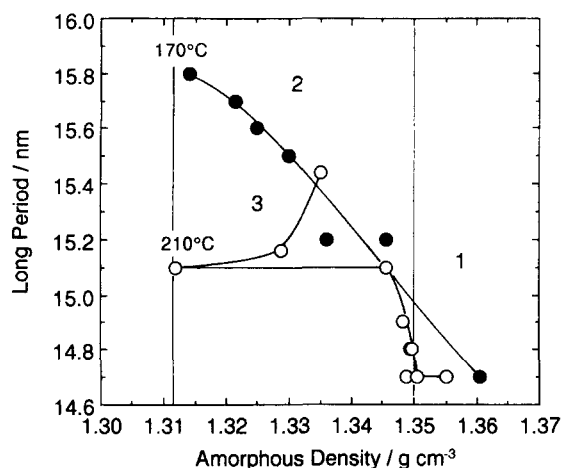


**Figure 4** Relationship between amorphous density ( $\rho_a$ ) and long period of PET annealed under dry (○) and wet (●) conditions

constant for annealed PET samples, the decrease in  $\rho_a$  indicated the increase in free volume in the amorphous region. The increasing ratio of free volume content with crystallization proceeding in region 2 was larger than that observed in region 1 for both annealing conditions.

Figure 4 shows the relationship between  $\rho_a$  and the long period of PET annealed under both conditions. For dry annealing conditions, the long period was almost constant around 14.7 nm in region 1; however, the long period increased from 14.7 to 15.1 nm with decreasing  $\rho_a$  in the narrow  $\rho_a$  range between 1.35 and 1.345 g cm<sup>-3</sup>, and levelled off at 15.1 nm in region 2, but increased again in region 3. On the other hand, the long period increased continuously with proceeding crystallization in regions 1 and 2 under wet annealing conditions. This result suggested that the lamellar thickening occurred because water absorbed in PET enhanced the segmental motion of the amorphous region of PET as reported previously<sup>11,20</sup>. Molecular chains in the amorphous region are supplied to thicken the lamellae. Therefore, the molecular chain supply from the amorphous region between lamellae to the crystal surface was restricted when the long period approached about 15.1 nm under the dry annealing condition. However, the amorphous region in which molecular motion was enhanced by absorbed water supplied amorphous molecules to the crystal surface to increase lamellar thickness under the wet annealing condition in region 2. For dry annealed samples,  $\rho_a$  decreased extremely without the change in long period in region 2. This result suggested that the amorphous structure changed without the increase in crystallinity on annealing in region 2 under the dry condition. On the contrary, the change in  $\rho_a$  correlated to that in the long period for wet annealed PET. These facts also suggested that the amorphous structure of the wet annealed PET differed from that of the dry annealed PET.

Figure 5 shows the relationship between  $\rho_a$  and the dynamic loss modulus ( $E''$ ) peak temperature of the  $\alpha$  relaxation of PET annealed under both conditions observed at 10 Hz. The  $E''$  peak temperature of the  $\alpha$  relaxation corresponded to the glass transition temperature ( $T_g$ ) at 10 Hz. For the dry annealing condition, the  $T_g$  was almost constant in region 1 and then decreased from 108 to 103°C in the narrow  $\rho_a$  range between 1.35 and 1.345 g cm<sup>-3</sup> and levelled off at about 103°C in

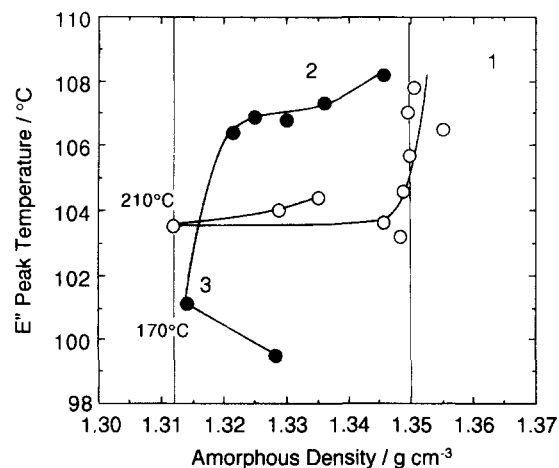


**Figure 5** Relationship between dynamic loss modulus ( $E''$ ) peak temperature of  $\alpha$  relaxation observed at 10 Hz and amorphous density ( $\rho_a$ ) of PET annealed under dry (○) and wet (●) conditions

region 2. The change in the long period induces the change in the amorphous structure and also  $T_g$  as previously described. Comparing with Figure 4, the  $T_g$  behaviour was similar to that of the long period for dry annealed PET. Considering the effect of the free volume content on  $T_g$ , the decrease in  $\rho_a$  gives a decrease in  $T_g$ . For dry annealed PET, however,  $T_g$  decreased in the narrow  $\rho_a$  range between 1.35 and 1.345 g cm<sup>-3</sup> and scarcely changed with decreasing  $\rho_a$  from 1.345 to 1.31 g cm<sup>-3</sup>; in other words,  $T_g$  was constant with increasing free volume content. In region 1, the  $T_g$  of PET decreased with increasing free volume content. Although  $\rho_a$  decreased remarkably in region 2, the  $T_g$  of PET was almost constant: 104 and 107°C for dry and wet annealing conditions, respectively. In region 2, the increase in free volume content no longer influenced the  $T_g$  of PET. The crystallinity increased in region 1<sup>11</sup>, but, on the other hand, the crystallinity scarcely increased and the qualitative amorphous structure change occurred in region 2. The excess free volume, which scarcely contributed to molecular motion, was produced by dry and wet annealing in region 2.

In region 2, wet annealing gave higher  $T_g$  than that of dry annealing at fixed  $\rho_a$ . This fact suggested that the amorphous structure of wet and dry annealing PET was different even at the same  $\rho_a$ . In fact, SAXS profiles of both annealing conditions were different. Details of these results will be reported in the near future.

Figures 6 and 7 show changes in the absorbance of absorption bands at 1042 and 848 cm<sup>-1</sup> of PET with  $\rho_a$  for PET annealed under dry and wet conditions, respectively. The absorbance of absorption bands at 1042 and 848 cm<sup>-1</sup> was normalized by the absorbance of absorption band at 795 cm<sup>-1</sup>. The absorption bands at 1042, 848 and 795 cm<sup>-1</sup> are assigned to the *gauche* and *trans* conformation and the orientation-sensitive bands characterized by the ethylene glycol linkage of PET, respectively<sup>21,22</sup>. Because the crystallinity scarcely increased under both annealing conditions in region 2<sup>11</sup>, the normalized absorbance of absorption bands at 1042 and 848 cm<sup>-1</sup> indicated the amount of *gauche* and *trans* conformation in the amorphous region of PET, respectively. For dry annealed PET, the *gauche* content of PET belonging to region 1, which was almost the same as that of the original PET ( $A_{1042 \text{ cm}^{-1}}/A_{795 \text{ cm}^{-1}} = 0.31$ ,

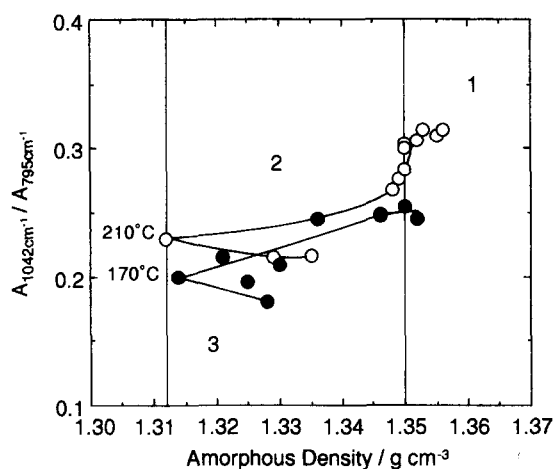


Figure 6 Changes in *gauche* conformation in PET annealed under dry (○) and wet (●) conditions as a function of amorphous density ( $\rho_a$ )

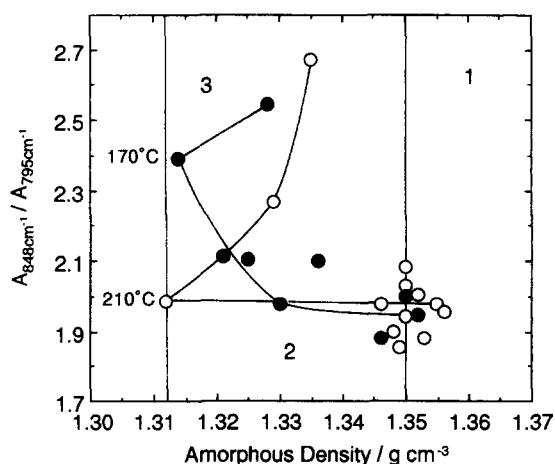


Figure 7 Changes in *trans* conformation in PET annealed under dry (○) and wet (●) conditions as a function of amorphous density ( $\rho_a$ )

$A$  = absorbance), scarcely changed with the proceeding crystallization. On the other hand, the wet annealed PET contained a lower *gauche* content compared with the original and the dry annealed PET, even if both annealed PETs showed the same *trans* content (Figure 7). Although the *trans* content scarcely changed with the decrease in  $\rho_a$  in region 2, the *gauche* content decreased continuously as a function of  $\rho_a$  for PET belonging to region 2 for both annealing conditions. The behaviour of the *gauche* content with  $\rho_a$  was similar to that of the long period. These facts suggested that the molecular conformation in the amorphous region changed from the *gauche* form to the extended form (such as tie molecules) with lamellar thickening. Kitamura *et al.*<sup>23</sup> reported that the *gauche* content of ethylenedioxy linkages in the amorphous region of PET fibres decreased with an increase in annealing temperature. As molecules in the amorphous region were drawn into the crystalline lamella during the lamellar thickening process, molecules in the amorphous region were considered to be extended. Under such a condition, tie molecular conformation of the amorphous chain changed from a random form to an extended form such as tie molecules between lamellae with proceeding lamellar thickening. The free volume content increased due to such conformational changes in

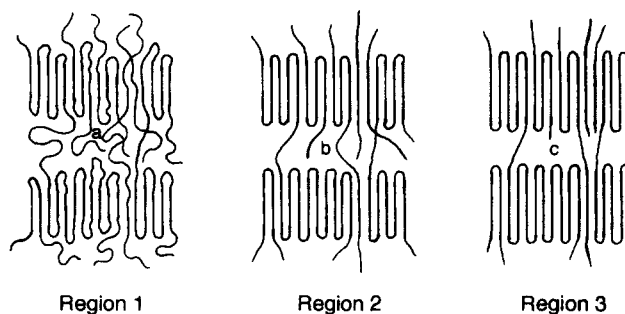


Figure 8 Schematic representation of model for microvoid formation: (a) ordinary amorphous region; (b) sparse amorphous region; (c) microvoid

the amorphous region between lamellae. The *gauche* content of samples decreased and the molecular conformation of the amorphous chain changed from a random form to an extended form in region 2 for both annealing conditions. As a result of perfection of the crystalline structure, the number of molecules in the amorphous region supposedly decreased. This is supported by the result reported in our previous paper<sup>11</sup> that the relaxation strength of the  $\alpha$  relaxation decreased with an increase in annealing temperature. Therefore, the amorphous structure became sparse and  $\rho_a$  decreased extensively following the conformational changes observed in region 2 for both annealing conditions. In region 3, the *gauche* content of samples decreased continuously even though  $\rho_a$  increased conversely.

As mentioned above, the qualitative amorphous structure change occurred in region 2, i.e. the excess free volume content, which scarcely contributed to molecular motion, increased by the conformational change in the amorphous chain. The excess free volume produced in region 2 might be converted to microvoids around  $1.31 \text{ g cm}^{-3}$  of  $\rho_a$ . After formation of microvoids from excess free volume in the amorphous region,  $\rho_a$  increased with proceeding crystallization because the *trans* conformation content of the amorphous chain was higher than that in region 2. For both annealing conditions, the excess free volume converted to microvoids at about  $1.31 \text{ g cm}^{-3}$  of  $\rho_a$ , corresponded to the maximum free volume content of amorphous PET molecules. The schematic model for microvoid formation due to annealing is shown in Figure 8. The process of the conversion from excess free volume to microvoids is now being examined by means of light scattering, SAXS and neutron scattering.

#### Dye uptake properties

In our previous papers<sup>11,12</sup> we reported the correlation between the dye uptake characteristics of PET films annealed under dry and wet conditions and their structure when they were dyed at  $130^\circ\text{C}$ . However, as PET films annealed under severe conditions were broken into small pieces during dyeing, the amorphous structure of PET in region 3 could not be discussed. In this study, dyeing temperature was set at  $110^\circ\text{C}$  to avoid breaking of samples annealed under a wide range of temperatures. The changes in dye uptake properties were discussed in detail in relation to the changes in amorphous structure due to annealing. Figure 9 shows the changes in dye exhaustion in PET in relation to the annealing temperature for PET annealed under dry and wet conditions.

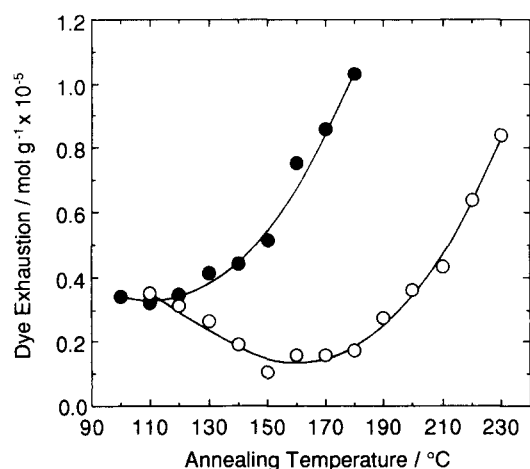


**Figure 9** Changes in dye exhaustion in PET annealed under dry (○) and wet (●) conditions as a function of annealing temperature

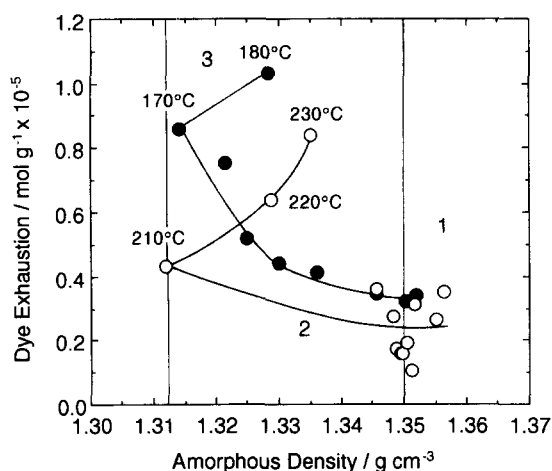


**Figure 10** Changes in dye exhaustion with amorphous density ( $\rho_a$ ) for PET annealed under dry (○) and wet (●) conditions

For dry annealed PET, the dye exhaustion decreased moderately, starting at 110°C and increasing at annealing temperatures above 190°C after passing the minimum at about 150°C. This dye uptake behaviour of the dry annealed PET film was similar to that of PET fibres<sup>1-4</sup>. A similar dye exhaustion tendency was observed in the case of the wet annealed PET, but the minimum dye exhaustion value appeared around 110°C. For samples annealed at a fixed temperature, the dye exhaustion in the wet annealed PET was larger than that in the dry annealed PET, demonstrating a large shift along the temperature scale.

The relationship between dye exhaustion and  $\rho_a$  for PET annealed under dry and wet conditions is shown in Figure 10. Although the amorphous density of PET decreased as shown in Figure 2, the dye exhaustion increased with decreasing  $\rho_a$  in region 2 for both annealing conditions. The dye exhaustion behaviour was influenced by quality change in the amorphous structure and by no means the amorphous fraction in PET. However, the dye exhaustion continuously increased with the converse increase in  $\rho_a$  in region 3 for both annealing conditions. These results suggested that a more open structure such as microvoids was formed by highly increased free volume under annealing conditions

corresponding to region 3, and dye molecules were absorbed in such a sparse amorphous region of PET.

The ratio of the absorbance of the  $\alpha$  band (600 nm) to that of the  $\beta$  band (560 nm) has been used as an indication of the degree of aggregation of the dye. It was reported that the value of the  $\alpha/\beta$  ratio was about 1.3 when most of the CV existed in monomeric form in the substrate and the ratio decreased with increasing degree of aggregation<sup>24</sup>. Figure 11 shows the changes in  $\alpha/\beta$  ratio with  $\rho_a$  of PET annealed under dry and wet conditions. The value of the  $\alpha/\beta$  ratio decreased with a decrease in  $\rho_a$  in region 1, but it was around 1.3 and dye molecules existed almost in monomeric form. In region 2, the dye exhaustion remarkably increased with increasing  $\rho_a$ , but the degree of aggregation hardly changed. The monomer and aggregate of the dye coexisted in this region. The  $\rho_a$  of PET increased again in region 3 by annealing above 210°C under dry conditions and above 170°C under wet conditions; however, the value of the  $\alpha/\beta$  ratio significantly decreased and the dye exhaustion remarkably increased and a greater part of the dye molecules existed in the aggregated state. Differences in the dye exhaustion and the degree of aggregation between the dry and wet annealed PET films were recognized at the same amorphous density. This is probably due to a difference in the amorphous structure and the molecular mobility of the polymer chain in the amorphous region between dry and wet annealing conditions.

Yonetake and co-workers<sup>9,10</sup> reported that disperse dyes were absorbed mainly on the side surfaces of lamellae using the mosaic-block structure model of crystalline polymers. If microvoids were produced from increased free volume content caused by conformational transformation from the *gauche* to the *trans* form with proceeding lamellar thickening and the dye absorbed into microvoids as an aggregated form, most of the absorbed dye should exist between lamellae. These results suggested that the free volume of PET increased as a result of a conformational change from the *gauche* to the *trans* form in amorphous molecules with increasing annealing temperature, whereas the amorphous structure became sparse and finally microvoid formation began at about 1.31 g cm<sup>-3</sup> of amorphous density. The dye uptake increased with increasing annealing temperature according to microvoid formation. The effect of the

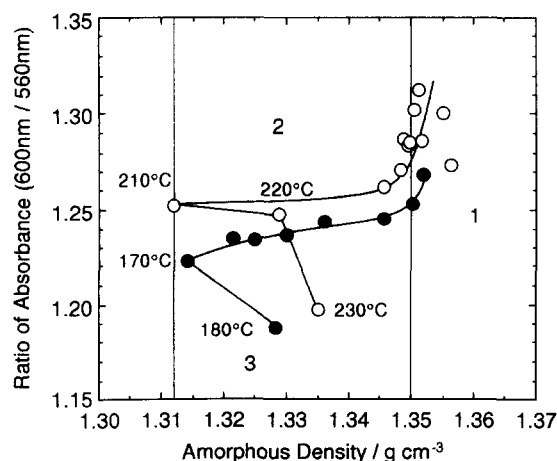


**Figure 11** Relationship between  $\alpha/\beta$  ratio and amorphous density ( $\rho_a$ ) for PET annealed under dry (○) and wet (●) conditions

annealing temperature on dye uptake behaviour consists of two opposing factors, i.e. a decrease in amorphous content (quantitative factor), decreasing the dye exhaustion, and an increase in free volume and microvoid content (qualitative factor), increasing the dye exhaustion and the degree of aggregation. The balance of these opposite effects can yield the minimum in dye uptake. The characteristic dyeing behaviour which was found by Marvin<sup>1</sup> was well explained in terms of quantitative and qualitative changes in the amorphous region.

## CONCLUSION

The amorphous structure change in PET induced by annealing under dry and wet conditions was studied in terms of  $\rho_a$  and dye uptake behaviour. From the mechanism of amorphous structure change, the amorphous structure was classified into the following three  $\rho_a$  regions. Region 1 ( $\rho_a > 1.35 \text{ g cm}^{-3}$ ); the amorphous fraction decreased with proceeding crystallization. The molecular conformation of the amorphous chain scarcely changed with crystallization, and the free volume content of the amorphous region scarcely increased with proceeding crystallization. The absorbed dye existed in monomeric form. Region 2 ( $1.35 \text{ g cm}^{-3} > \rho_a > 1.31 \text{ g cm}^{-3}$ ); the molecular conformation of the amorphous chain changed from the *gauche* to the *trans* form. The free volume content of the amorphous region greatly increased with crystallization. The absorbed dye existed as a mixture of monomeric form and aggregated form. Region 3 ( $\rho_a > 1.31 \text{ g cm}^{-3}$ ); the  $\rho_a$  value increased conversely with proceeding crystallization. The increased free volume converted to microvoids at  $1.31 \text{ g cm}^{-3}$  of  $\rho_a$ . Most of the absorbed dyes existed in aggregated form. Compared with the dry annealing condition, regions 1–3 of PET annealed under wet conditions were observed at lower annealing temperatures. The mechanism of the amorphous structure change in each region was almost the same for both annealing conditions; however, the

amorphous structure difference existed in region 2 between dry and wet conditions.

## REFERENCES

1. Marvin, D. N., *J. Soc. Dyers Colour.*, 1954, **70**, 16.
2. Andriessen, J. and Soest, J. V., *Textilveredlung*, 1968, **3**, 618.
3. Mitsuishi, Y. and Tonami, H., *Sen-i Gakkaishi*, 1963, **19**, 140.
4. Dumbleton, J. H., Bell, J. P. and Murayama, T., *J. Appl. Polym. Sci.*, 1968, **12**, 2491.
5. Gupta, V. B., Kumar M. and Gulrajani, M. L., *Text. Res. J.*, 1975, **45**, 463.
6. Warwicker, J. O., *J. Soc. Dyers Colour.*, 1972, **88**, 142.
7. Huisman, R. and Heuvel, M., *J. Appl. Polym. Sci.*, 1978, **22**, 943.
8. Sakai, T., Miyasaka, K. and Ishikawa, K., *Sen-i Gakkaishi*, 1978, **34**, T-475.
9. Masuko, T. S., Hasegawa, Yonetake, K. and Karasawa, M., *Makromol. Chem.*, 1981, **182**, 2049.
10. Yonetake, K., Masuko, T., Shimanuki T. and Karasawa, M., *J. Appl. Polym. Sci.*, 1983, **28**, 3049.
11. Toda, T., Yoshida, H. and Fukunishi, K., *Polymer*, 1995, **36**, 699.
12. Toda, T., Yoshida, H. and Fukunishi, K., *Sen-i Gakkaishi*, 1994, **50**, 599.
13. Toda, T. and Hida, M., *Sen-i Gakkaishi*, 1990, **46**, 155.
14. Wunderlich, B., *Macromolecular Physics*, Vol. 1. Academic Press, New York, 1973, p. 389.
15. Sakaguchi, N., Oda, T., Nakai, A. and Kawai, H., *Sen-i Gakkaishi*, 1977, **33**, T-499.
16. Santa Cruz, C., Balta Calleja, F. J., Zachmann, H. G., Stribeck, N. and Asano, T., *J. Polym. Sci., Polym. Phys. Edn*, 1991, **29**, 819.
17. Balta Calleja, F. J., Santa Cruz, C. and Asano, T., *J. Polym. Sci., Polym. Phys. Edn*, 1993, **31**, 557.
18. Groeninckx, G., Reynaers, H., Berghans, H. and Smets, G., *J. Polym. Sci., Polym. Phys. Edn*, 1980, **18**, 1311.
19. Fontaine, F., Lendent, J., Groeninckx, G. and Reynaers, H., *Polymer*, 1982, **23**, 185.
20. Toda, T., Yoshida, H. and Hida, M., *Sen-i Gakkaishi*, 1992, **48**, 84.
21. Schmidt, P. G., *J. Polym. Sci., Part A*, 1963, **1**, 1271.
22. Miyake, A., *J. Polym. Sci.*, 1959, **38**, 479.
23. Kitamura, K., Shibata, F. and Yoshida, Z., *Sen-i Gakkaishi*, 1971, **27**, 359.
24. Nakamura, R. and Hida, M., *Sen-i Gakkaishi*, 1983, **39**, T-12.